

CANCER

A precision therapy against cancers driven by *KIT*/*PDGFRA* mutations

Erica K. Evans,¹ Alexandra K. Gardino,¹ Joseph L. Kim,¹ Brian L. Hodous,¹ Adam Shutes,¹ Alison Davis,¹ Xing Julia Zhu,¹ Oleg Schmidt-Kittler,¹ Doug Wilson,¹ Kevin Wilson,¹ Lucian DiPietro,^{1*} Yulian Zhang,^{1†} Natasja Brooijmans,¹ Timothy P. LaBranche,¹ Agnieszka Wozniak,² Yemarshet K. Gebreyohannes,² Patrick Schöffski,² Michael C. Heinrich,³ Daniel J. DeAngelo,⁴ Stephen Miller,¹ Beni Wolf,¹ Nancy Kohl,^{1‡} Timothy Guzi,¹ Nicholas Lydon,¹ Andy Boral,¹ Christoph Lengauer^{1§}

Copyright © 2017
The Authors, some
rights reserved;
exclusive licensee
American Association
for the Advancement
of Science. No claim
to original U.S.
Government Works

Targeting oncogenic kinase drivers with small-molecule inhibitors can have marked therapeutic benefit, especially when administered to an appropriate genomically defined patient population. Cancer genomics and mechanistic studies have revealed that heterogeneous mutations within a single kinase can result in various mechanisms of kinase activation. Therapeutic benefit to patients can best be optimized through an in-depth understanding of the disease-driving mutations combined with the ability to match these insights to tailored highly selective drugs. This rationale is presented for BLU-285, a clinical stage inhibitor of oncogenic *KIT* and *PDGFRA* alterations, including activation loop mutants that are ineffectively treated by current therapies. BLU-285, designed to preferentially interact with the active conformation of *KIT* and *PDGFRA*, potently inhibits activation loop mutants *KIT* D816V and *PDGFRA* D842V with subnanomolar potency and also inhibits other well-characterized disease-driving *KIT* mutants both in vitro and in vivo in preclinical models. Early clinical evaluation of BLU-285 in a phase 1 study has demonstrated marked activity in patients with diseases associated with *KIT* (aggressive systemic mastocytosis and gastrointestinal stromal tumor) and *PDGFRA* (gastrointestinal stromal tumor) activation loop mutations.

INTRODUCTION

Targeted inhibition of oncogenic kinases has transformed the care of a subset of cancer patients whose malignancy is driven by activating mutations and thus vulnerable to therapeutic inhibition of the activated oncoprotein. Successful examples of this approach include erlotinib and crizotinib for mutant *EGFR*- and *ALK*-/*ROS*-driven lung cancers, respectively (1–3), vemurafenib for mutant *BRAF* melanomas (4), and imatinib for both *BCR-ABL*-driven chronic myeloid leukemia and *KIT* mutant gastrointestinal stromal tumor (GIST) (5, 6). However, effectively inhibiting a disease-driving kinase is complicated because various mechanisms of kinase activation, including alteration of conformational states or changes in dimerization potential, influence kinase inhibitor binding. Evaluation of individual oncogenic mutations is therefore critical to effectively pair an unmet medical need with the design of an appropriately targeted agent.

The *KIT* receptor belongs to the class III receptor tyrosine kinase (RTK) family that also includes the structurally related proteins *PDGFRA* (platelet-derived growth factor receptor A), *PDGFRB*, *FLT3* (FMS-like tyrosine kinase 3), and *CSF1R* (colony-stimulating factor 1 receptor). Normally, stem cell factor (SCF) binds to and activates *KIT* by inducing dimerization, autophosphorylation, and initiation of downstream signaling (7). In several tumor types, however, somatic activating mutations in *KIT* drive ligand-independent constitutive activity; these mutations have been most extensively studied in GIST (8, 9).

Nearly 80% of metastatic GISTs have a primary activating mutation in either the extracellular region (exon 9) or the juxtamembrane (JM) domain (exon 11) of *KIT*, and up to an additional 10% are mutated in the highly related kinase *PDGFRA* (10). The recognition that many *KIT* mutant tumors respond to treatment with imatinib has transformed the treatment of GIST. First-line imatinib treatment provides a median progression-free survival (PFS) of 18 to 24 months (11). However, most GIST patients eventually relapse due to a secondary mutation in *KIT* that markedly decreases the binding affinity of imatinib. These resistance mutations invariably arise within the adenosine 5'-triphosphate (ATP)-binding pocket (exons 13 and 14) or the activation loop (exons 17 and 18) of the kinase (8). Activation loop mutations accumulate with increasing frequency after second-line therapy (sunitinib), which also has inadequate activity on activation loop mutant proteins (12, 13). In 5 to 6% of unresectable or metastatic GIST patients, an activation loop mutation in *PDGFRA* at amino acid 842 occurs as the primary mutation (14, 15) and is insensitive to imatinib and all other approved GIST agents (16, 17). With no effective treatments available, the prognosis for patients with metastatic *PDGFRA* D842V GIST is particularly dire, with PFS of only 3 to 5 months and overall survival of 15 months (16, 18).

Beyond GIST, the D816V mutant in the activation loop of *KIT*, which is structurally identical to the D842V mutant in *PDGFRA* (15), is found in more than 90% of patients (19, 20) with systemic mastocytosis (SM), a rare hematologic disease of clonal mast cells (21). In advanced forms of SM, organ function is compromised by the accumulation of excess mast cells, and overall survival is decreased. Although the indolent subtype of the disease does not affect survival, many patients suffer from debilitating symptoms associated with mast cell degranulation, histamine release, and a reduced quality of life. Midostaurin has recently been approved by the U.S. Food and Drug Administration (FDA) for the treatment of advanced SM,

¹Blueprint Medicines, Cambridge, MA 02139, USA. ²Laboratory of Experimental Oncology, Department of Oncology, KU Leuven, Belgium 3000. ³VA Health Care System and Knight Cancer Institute, Oregon Health and Science University, Portland, OR 97239, USA. ⁴Department of Medical Oncology, Dana-Farber Cancer Institute, Boston, MA 02215, USA.

*Present address: Relay Therapeutics, Cambridge, MA 02142, USA.

†Present address: Actinium Pharmaceuticals Inc., New York, NY 10016, USA.

‡Present address: Nancy Kohl Consulting, Wellesley, MA 02482, USA.

§Corresponding author. Email: clengauer@blueprintmedicines.com

but whether its mechanism of action relies upon KIT D816V inhibition is unclear (22).

We embarked on an in-depth mechanistic evaluation of KIT/PDGFR α -directed small-molecule inhibitors across a comprehensive collection of clinically relevant KIT primary and resistance mutants. The results of these studies illustrate a continuum of activation states for KIT mutants. This understanding has guided the discovery and development of BLU-285, a highly potent and selective small-molecule inhibitor of KIT and PDGFR α activated mutants. BLU-285 demonstrated robust in vitro and in vivo activity in various KIT-driven pre-clinical models and has provided promising initial clinical activity in patients with GIST and SM.

RESULTS

KIT activation loop mutants display affinity for type I inhibitors

Inhibitors that bind to the inactive conformation of kinases are categorized as type II inhibitors (23), and the three agents currently FDA-approved for the treatment of GIST (imatinib, sunitinib, and regorafenib) share this binding mode. The ability of type II inhibitors to suppress exon 9 and 11 KIT mutants (24, 25) indicates that these alterations provide only a minor shift in equilibrium in favor of the active over the inactive conformation of the kinase (26, 27). In contrast, mutations in the activation loops of KIT and PDGFR α induce a more prominent equilibrium shift toward the active conformation, which is incompatible with type II inhibitor binding (26). We therefore pursued a strategy to develop a selective type I inhibitor or an active conformation inhibitor of KIT and PDGFR α to address activation loop mutants.

Analysis of screening data against a panel of wild-type (WT) and mutant KIT proteins with a set of commercial and proprietary kinase-directed small-molecule inhibitors revealed not only the binding of type I scaffolds to the D816V activation loop mutant but also to the V559D exon 11 JM domain mutant and to KIT WT proteins (fig. S1). As anticipated, type II inhibitors displayed poor affinity for the D816V mutant. To extend our understanding of type I versus type II inhibitor binding preferences across a larger spectrum of clinically relevant KIT mutants, an additional exon 11 mutant (V560G), as well as several exon 17 and 18 activation loop mutants (D816E, D820E, and A829P), were added to the evaluation (Fig. 1). Binding data analysis confirmed that KIT WT does not demonstrate a strong preference for one inhibitor type over the other, although it does show marked sensitivity to some type II inhibitors. The KIT V560G mutant bound tightly to type II inhibitors, whereas KIT activation loop mutants (D816E, D816V, D820E, and A829P) displayed either a slight bias toward or a pronounced affinity for type I inhibitors. Notably, the KIT D816V mutant consistently displayed a marked preference for type I inhibitors over that of type II inhibitors. These data validated a focus on type I inhibitors for suppressing KIT D816V activity and additional activation loop mutants and also provided an explanation for the difficulty that previous drug discovery efforts have encountered when focused on type II molecules for activation loop inhibition.

BLU-285 is a potent and selective inhibitor of KIT and PDGFR α activation loop mutants

Extensive exploration of diverse chemical scaffolds against the mutant KIT panel coupled with optimization of drug metabolism and pharmacokinetic properties yielded BLU-285 (Fig. 2A). BLU-285 demonstrated exquisite activity on KIT activation loop mutants, with biochemical IC₅₀ measured in the subnanomolar range for all activation loop mutants

tested including KIT D816V (IC₅₀ = 0.27 nM) and PDGFR α D842V (IC₅₀ = 0.24 nM) (Fig. 2B). Broad screening against a large panel of human kinases at 3 μ M revealed that BLU-285 had very limited potential for activity outside of KIT and PDGFR α . BLU-285 was also more than 150-fold more potent on KIT D816V than several important kinase antitargets such as VEGFR2 (vascular endothelial growth factor receptor 2), SRC, and FLT3 (Fig. 2C and tables S1 and S2). This large difference in BLU-285 activity between KIT D816V and other kinases suggested that off-target inhibition in vivo would be unlikely and that BLU-285 was a highly selective inhibitor of KIT and PDGFR α activation loop mutants.

Comparatively, the type II inhibitors imatinib, sunitinib, and regorafenib only weakly inhibited KIT D816V or PDGFR α D842V enzyme activity (Fig. 2B). Of these approved agents for GIST, the overall kinase selectivity profile of BLU-285 was most similar to imatinib (Fig. 2C), which has an impressive tolerability profile in the clinic relative to the others (5, 6, 28). Type I inhibitors midostaurin and crenolanib, an investigational compound in clinical trials for the treatment of GIST patients with primary PDGFR α D842 mutations (29), registered biochemical activity against the activation loop mutants in the low-digit nanomolar range. However, both showed extensive activity across the human kinome, which may be associated with a more complex safety profile in the clinic and a smaller therapeutic window (Fig. 2C).

BLU-285 is active across a spectrum of clinically observed KIT mutants

To assess the breadth of activity of BLU-285 against KIT mutations identified in patients, we tested BLU-285 biochemically against a large panel of KIT primary and acquired resistance mutants representing various diseases and stages of progression. BLU-285 demonstrated potency across a spectrum of KIT mutants and superior potency to imatinib on all mutants tested, revealing broad potential for this type I inhibitor in GIST (Fig. 3). Activity was greatest against the KIT exon 11/17 (V560G/D816V) double mutant (Fig. 3). Mutations in the JM domain and activation loop each serve to release autoinhibitory conformations of the kinase domain (26), and together, they may virtually lock in the active kinase conformation to which BLU-285 preferentially binds, thereby enhancing its potency. Other KIT activation loop mutants showed sensitivity to BLU-285 with IC₅₀ < 2 nM, reflecting a strong bias of these mutants for the active kinase conformation. BLU-285 also demonstrated low nanomolar potency against JM domain mutants, suggesting that exon 11 mutations in KIT-driven GIST are sensitive to both type I and type II inhibitors.

ATP-binding site mutations in KIT exons 13 (V654A) and 14 (T670I), which cause resistance to imatinib, were less sensitive to BLU-285, signifying preference for a WT ATP-binding site for optimal compound binding. However, like the KIT activation loop mutants, both ATP site mutants were more sensitive to BLU-285 inhibition in the presence of JM domain mutants as compared to the ATP site mutants alone (Fig. 3). These findings further reinforce the positive effect of JM domain mutants on BLU-285 accessibility to the active conformation of the enzyme. Finally, BLU-285 showed greater potency against all disease-relevant KIT mutants than against KIT WT.

BLU-285 is highly active in KIT mutant cell lines

To confirm the activities observed in biochemical assays, we used KIT-driven cell lines to assess BLU-285 target engagement (Table 1).

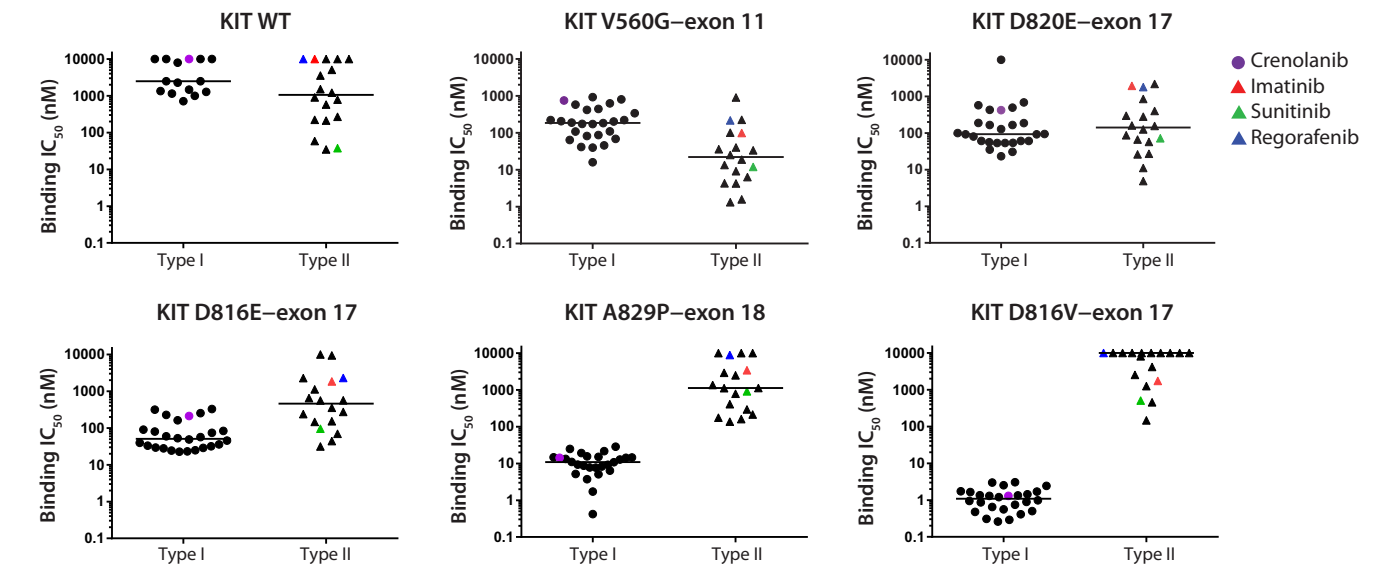


Fig. 1. Inhibitor binding analysis reveals type I preference for KIT activation loop mutants. Half-maximal inhibitory concentration (IC_{50} ; in nanomolar) of type I (15 for KIT WT and 26 for mutant KIT) and 18 type II compounds bound to various KIT proteins as measured by LanthaScreen in the absence of ATP. Median values are depicted by horizontal lines. Reference compounds are depicted as follows: imatinib, red triangle; sunitinib, green triangle; regorafenib, blue triangle; crenolanib, purple circle).

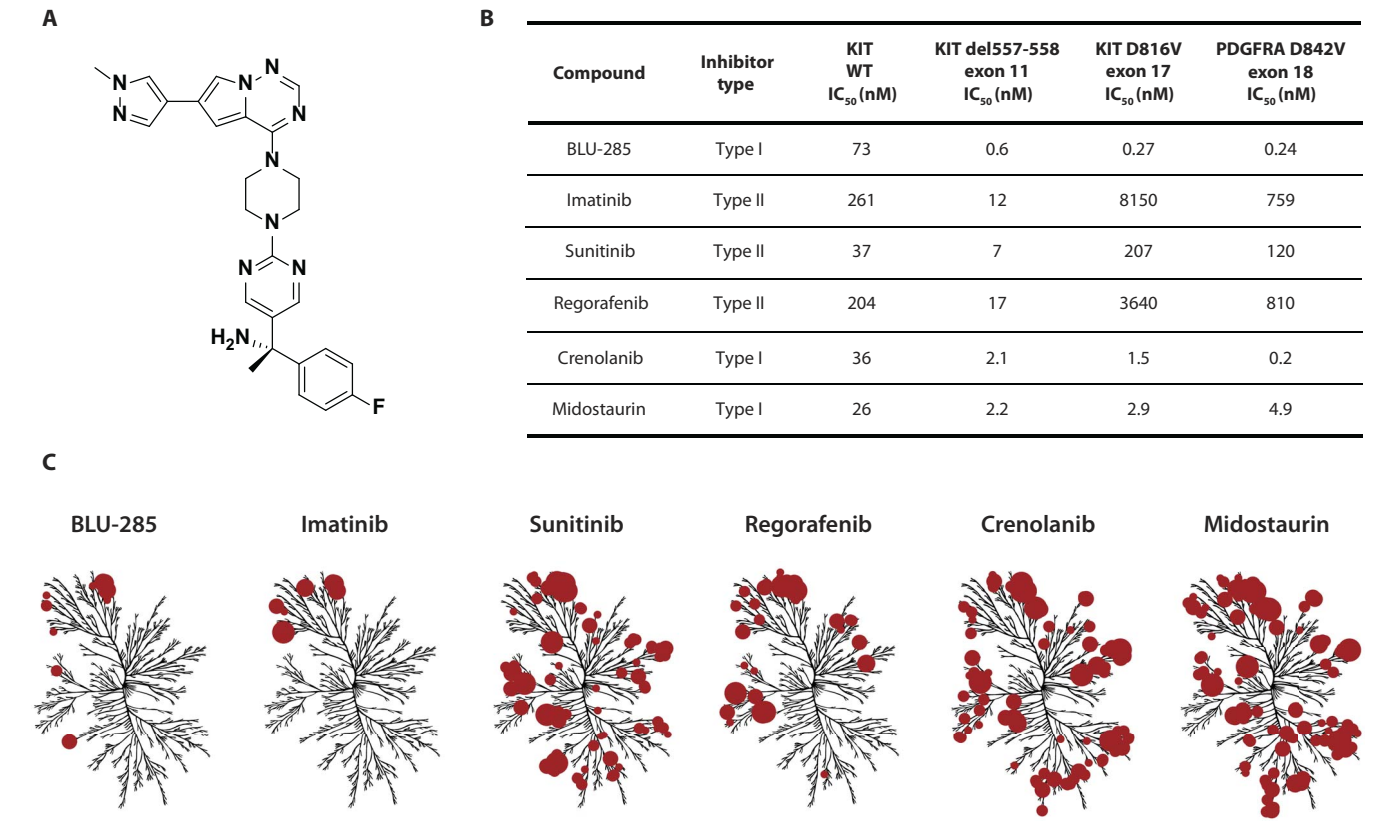


Fig. 2. BLU-285 is a potent and highly selective inhibitor of KIT and PDGFRA activation loop mutants. (A) Chemical structure of BLU-285. (B) Biochemical potency against KIT WT and the KIT del557-558 (exon 11), D816V (exon 17), and PDGFRA D842V (exon 18) mutants for BLU-285 and several compounds in use or being explored for the treatment of GIST and SM. (C) Binding data for compounds screened at 3 μ M against 392 kinases are depicted as red circles on the kinome tree. The size of the circle indicates binding potency. Kinome illustration reproduced courtesy of Cell Signaling Technology (www.cellsignal.com).

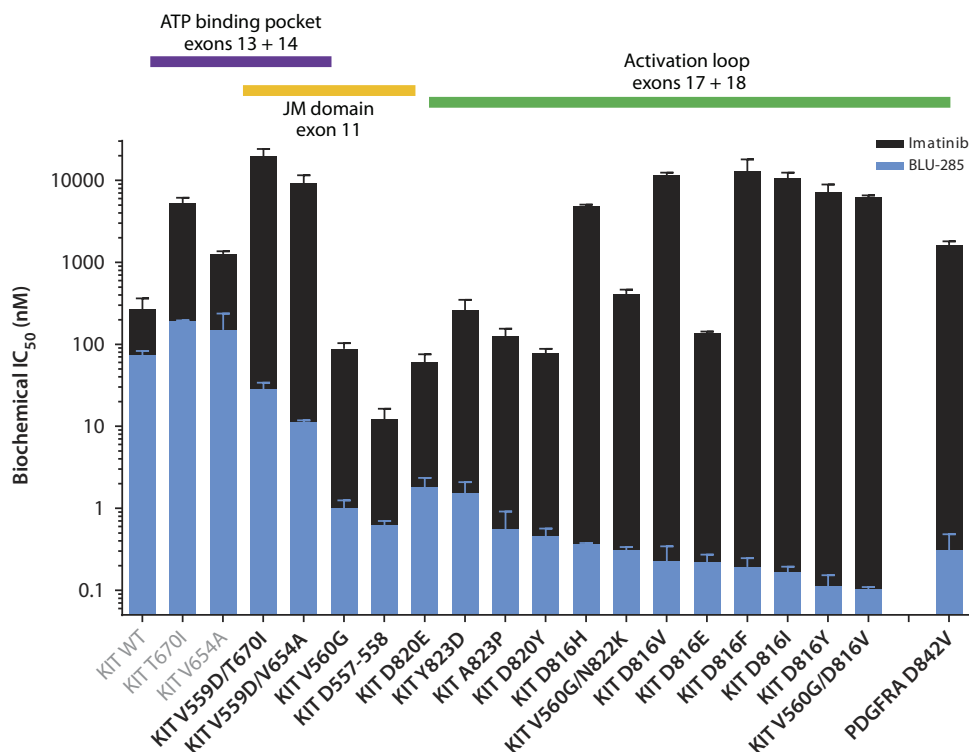


Fig. 3. BLU-285 is active against a spectrum of KIT and PDGFRA disease-relevant mutants. Biochemical data highlights BLU-285 activity across 19 KIT and PDGFRA mutant proteins. Data are depicted as bars that represent the mean IC_{50} value + SD for BLU-285 (light blue) and imatinib (black). Clinically observed KIT and PDGFRA mutants are clustered by their location within the primary protein sequence. The exon location and associated structural region for each mutant are listed above, and disease relevant mutants are shown in bold.

The most marked effect was seen in HMC1.2 cells, which carry the dual exon 11/17 (V560G/D816V) *KIT* mutations (30). BLU-285 potently inhibited both *KIT* autophosphorylation (IC_{50} = 4 nM) and downstream signaling in this cell line (Table 1 and fig. S2). BLU-285 was also highly active on the murine *KIT* D814Y mutant (equivalent to human D816Y) mastocytoma line P815 (IC_{50} = 22 nM) and on *KIT* exon 17 N822K in the human Kasumi-1 acute myeloid leukemia line (IC_{50} = 40 nM; Table 1) (31, 32). BLU-285 inhibited autophosphorylation in the HMC1.1 cell line expressing the *KIT* JM domain V560G mutant (IC_{50} = 100 nM) but with less potency than that observed in *KIT* exon 17 mutant cell lines. Finally, BLU-285 showed the weakest activity against *KIT* WT, inhibiting autophosphorylation with an IC_{50} of 192 nM in SCF-stimulated M-07e human megakaryoblastic leukemia cells, pointing to a potential safety margin for inhibition of mutant *KIT* over endogenous *KIT* WT signaling and other class III RTKs.

Antiproliferative effects of BLU-285 in *KIT*-dependent cell lines correlated well with on-target potencies against individual *KIT* mutants (Table 1). Together, these in vitro cellular data reflected the biochemical activity of BLU-285 on *KIT* mutant and WT enzymes, where BLU-285 potency correlated with the activation status of the enzyme. A similar pattern was observed with PDGFRA in which cellular potency tracked with biochemical activity and the activated state of the protein; BLU-285 was most potent against the PDGFRA D842V activation loop mutant, which distinguished this compound from other established agents used for the treatment of GIST (Table 1 and fig. S3).

BLU-285 demonstrates antitumor activity in preclinical models of *KIT*-driven diseases

In vivo activity of BLU-285 was assessed across a panel of *KIT*-driven disease models. The P815 mastocytoma cell line was used to establish a *KIT* mutant exon 17 subcutaneous allograft model. BLU-285, administered orally, once daily from 0.3 to 30 mg/kg, exhibited dose-dependent antitumor activity in this model (Fig. 4A). BLU-285 was well tolerated at all doses, showing no adverse effects on body weight (Fig. 4B). Dasatinib, used at the maximum tolerated dose (MTD) in vivo as a comparator based on its reported biochemical activity against multiple *KIT* D816 mutants (33), demonstrated inferior activity compared to BLU-285, likely due to its poor pharmacokinetics and issues with tolerability (Fig. 4B) (34). Pharmacokinetic and pharmacodynamic (PK/PD) analyses of plasma exposure and target engagement in tumor samples showed that phospho-*KIT* (pKIT) inhibition could be sustained over 24 hours (Fig. 4C and fig. S4). BLU-285 at a 10 mg/kg dose caused 75% pKIT inhibition with significant antitumor activity [P < 0.001, analysis of variance (ANOVA)], whereas BLU-285 at 30 mg/kg drove sustained pKIT inhibition to 90% and led to full tumor regression

(table S3). These data demonstrated that complete target coverage by BLU-285 was achievable at exposures that were well tolerated.

Next, the activity of BLU-285 was assessed in a patient-derived xenograft (PDX) from a refractory GIST lesion bearing *KIT* exon 11/17 (del557-558/Y823D) alterations. As anticipated, this model was resistant to imatinib (Fig. 4D, top). These data are reflective of the clinical experience because patients with this *KIT* exon 11/17 double mutation usually progress on imatinib and sunitinib therapies, leaving regorafenib as their final approved therapeutic option. Administration of regorafenib (30 mg/kg), equivalent to the recommended human dose of 160 mg (35), resulted in tumor stasis in this model, as did BLU-285 (3 mg/kg). In contrast, BLU-285 at doses of 10 and 30 mg/kg resulted in tumor regression (Fig. 4D, top) and were well tolerated (fig. S5). Pharmacodynamic analysis of tumors harvested 24 hours after BLU-285 administration revealed a dose-dependent inhibition of *KIT* autophosphorylation correlating with tumor response (Fig. 4D). Microscopic evaluation showed that in addition to decreases in tumor size, the BLU-285 (10 and 30 mg/kg) cohorts exhibited 27 and 50% reductions in nuclear density (fig. S6). This decrease resulted from myxoid degeneration, a phenomenon observed in GIST and select other mesenchymal tumors, which is characterized by replacement of tumor cells by connective tissue mucosubstances. Myxoid degeneration is known to occur in GIST tumors responding to imatinib or undergoing spontaneous regression (10, 36).

The potent activity of BLU-285 toward *KIT* exon 11 JM domain mutants in the biochemical and cellular settings warranted preclinical

Table 1. Inhibition of KIT/PDGFRα autophosphorylation and proliferation in cell lines.

Cell line	Mutation	Exon	Tissue	pKIT inhibition IC ₅₀ (nM)			
				BLU-285	Imatinib	Sunitinib	Regorafenib
M-07e	KIT WT	—	Human megakaryoblastic leukemia	192	336	3	63
HMC1.1	KIT V560G	11	Human mast cell leukemia	100	21	1	38
Kasumi	KIT N822K	17	Human acute myeloid leukemia	40	129	6	111
P815	KIT D816Y	17	Murine mastocytoma	22	1236	611	128
HMC1.2	KIT V560G/D816V	11/17	Human mast cell leukemia	4	9144	14,488	314
CHO	PDGFRA WT	—	Engineered	95	<100		
CHO	PDGFRA V561D	12	Engineered	40	<100		
CHO	PDGFRA D842V	18	Engineered	30	3145		
Cell line	KIT mutation	Exon	Tissue	Proliferation IC ₅₀ (nM)			
				BLU-285	Imatinib	Sunitinib	Regorafenib
M-07e	WT	—	Human megakaryoblastic leukemia	417	604	132	678
HMC1.1	V560G	11	Human mast cell leukemia	344	36	13	115
Kasumi	N822K	17	Human acute myeloid leukemia	75	382	31	211
P815	D816Y	17	Murine mastocytoma	202	2,811	230	1,974
HMC1.2	V560G/D816V	11/17	Human mast cell leukemia	125	11,355	1506	>25,000

exploration in a model of primary GIST bearing the *KIT* exon 11 del557-559insF alteration. This PDX model was sensitive to imatinib, as expected (Fig. 4E, top). Notably, doses of 30 and 100 mg/kg BLU-285 led to tumor regression similar to that observed with imatinib, and at 10 mg/kg, BLU-285 produced tumor stasis. Again, histological assessment of tumors showed a decrease in cellularity and myxoid degeneration in the imatinib and BLU-285 treatment groups, coincident with tumor regression (fig. S7). Therefore, although BLU-285 was most potent in the *KIT* activation loop mutant models, robust in vivo activity against the primary *KIT* exon 11 GIST mutants was achieved at slightly higher yet well-tolerated exposures (fig. S8). Assuming similar dose-exposure tolerability in patients, these results suggest that in addition to activity on activation loop mutants alone and the exon 11/17 double mutants in refractory GIST, BLU-285 may be able to prevent the emergence of the primary *KIT* exon 11 mutant clone in the clinical setting of acquired resistance.

Finally, a GIST PDX model bearing the *KIT* exon 11/13 (del557-558/V654A) double mutation was studied. This model was resistant to imatinib and sensitive to sunitinib as expected (Fig. 4F, top). A dose of BLU-285 (10 mg/kg) was not efficacious, reflecting the reduced activity of BLU-285 against this *KIT* exon 11/13 (V559D/V654A) double mutant observed biochemically (Fig. 3). In contrast, BLU-285 at the dose of 30 mg/kg resulted in marked tumor regression, concomitant with roughly 60% inhibition of *KIT* autophosphorylation (Fig. 4F, bottom). These results confirm a dose-dependent in vivo activity of BLU-285 against *KIT* exon 11/13 lesions, suggesting broad activity of BLU-285 across the clinically relevant *KIT* mutational spectrum observed in GIST.

BLU-285 exhibits clinical activity in early studies

To investigate the impact of BLU-285 on *KIT*- and *PDGFRA*-driven malignancies, we progressed BLU-285 into phase 1, first-in-human (FIH) dose-escalation studies in patients with advanced, unresectable GIST (NCT02508532) and advanced SM (NCT02561988). These two patient populations lack effective therapies and are each characterized by a high incidence of *KIT* and/or *PDGFRA* activation loop mutations.

A 65-year-old female with primary gastric *PDGFRA* D842V mutant GIST, who had progressed on previous imatinib, dasatinib, and crenolanib therapy, was enrolled at the first dose level (30 mg) (37). BLU-285 was administered orally, once daily in cycles of 28 days, and radiographic response was assessed per Response Evaluation Criteria in Solid Tumors (RECIST1.1) on day 1 of cycle 3. After 8 weeks of treatment with BLU-285, a 31% reduction in tumor size was observed by computed topography (CT) scan and confirmed by central radiographic review (Fig. 5A). A second CT scan 2 months later confirmed a partial response with 48% reduction in tumor size, and response was maintained for at least 15 cycles and continued at the time of manuscript preparation. Interrogation of circulating tumor DNA (ctDNA) collected before and at 2-week intervals after BLU-285 administration demonstrated a rapid and sustained reduction of *PDGFRA* D842V allele burden detected in the plasma (Fig. 5A).

Similar early antitumor activity was observed in a 48-year-old patient with a GIST tumor bearing a rare primary *KIT* D820Y activation loop mutation with clinical progression on previous imatinib, sunitinib, and regorafenib therapy (37). This patient was treated once daily with 60 mg of BLU-285; RECIST1.1 evaluation revealed a 25% tumor shrinkage at the first assessment that was confirmed on day 1 of cycle 5, with a

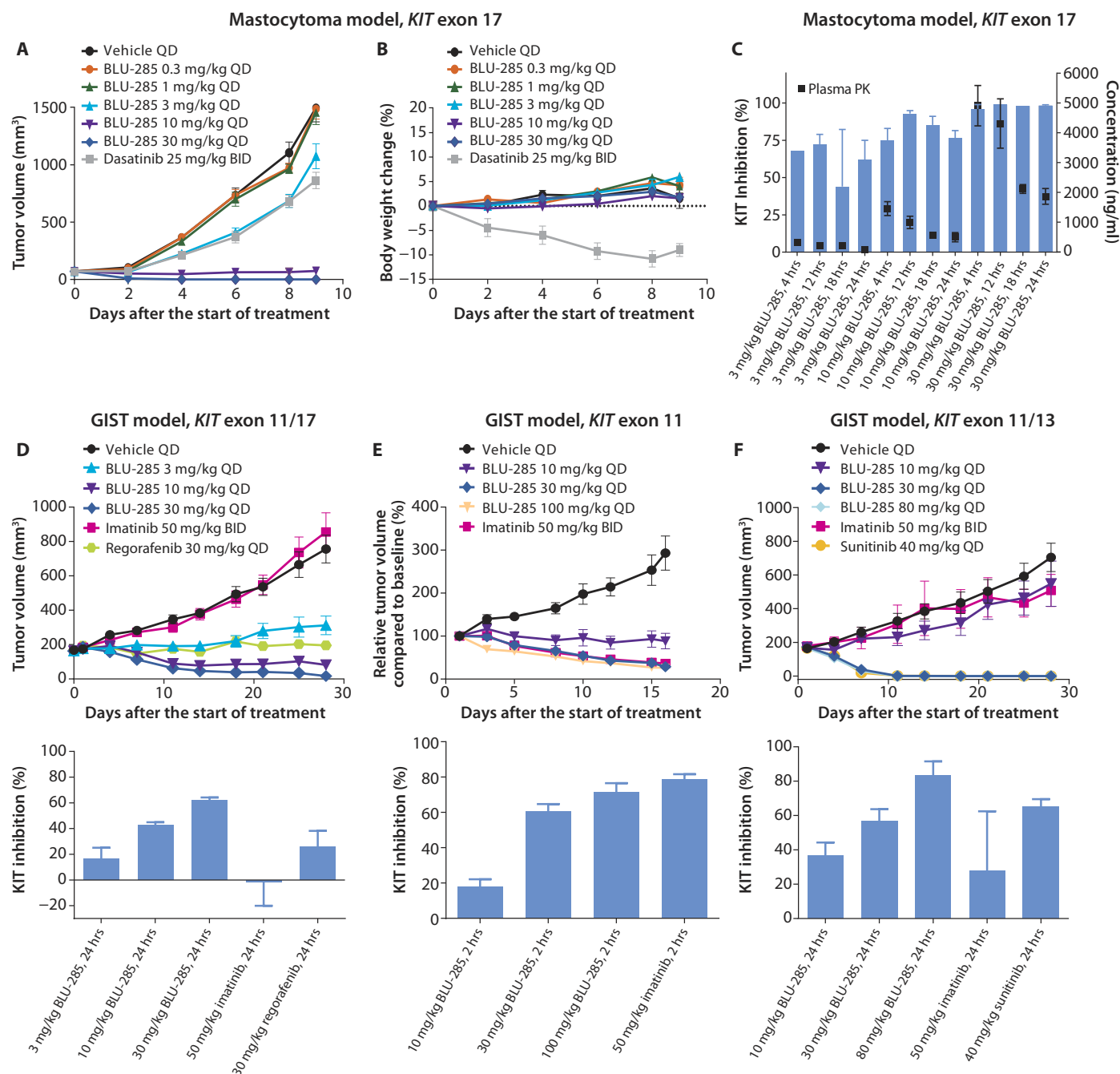


Fig. 4. BLU-285 demonstrates antitumor activity across multiple KIT-driven in vivo disease models. BLU-285 antitumor activity in both primary and refractory KIT-driven disease models. (A to C) Antitumor activity (A), body weight (B), and PK/PD (C) relationship for BLU-285 and dasatinib in a P815 KIT D814Y mastocytoma allograft model. (D to F) Antitumor activity of BLU-285 and reference compounds (top) and pharmacodynamic analysis of KIT inhibition (bottom) in human GIST PDX models of disease with (D) KIT exon 11/17 delW557K558/Y823D, (E) KIT exon 11 delW557-V559insF, and (F) KIT exon 11/13 delW557K558/V654A mutations. QD, once daily; BID, twice daily.

28% reduction and maintained through cycle 15 (32% reduction), as assessed by central radiographic review (Fig. 5B).

Finally, in advanced SM, robust clinical activity was observed in a patient treated with 60 mg of BLU-285 (38). Bone marrow mast cell infiltration, a hallmark of SM, was measured at baseline and again after two cycles of BLU-285. A marked decrease in bone marrow mast cells

was observed, indicating an effect on aberrant mast cell survival within the bone marrow environment and suggestive of rapid therapeutic activity (Fig. 5C). This early activity of BLU-285 on both GIST and SM with *PDGFRA* and *KIT* activation loop mutations suggests the promise of this targeted therapy for several typically treatment refractory patient populations.

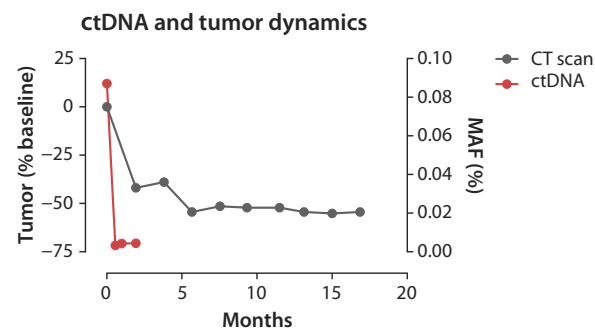
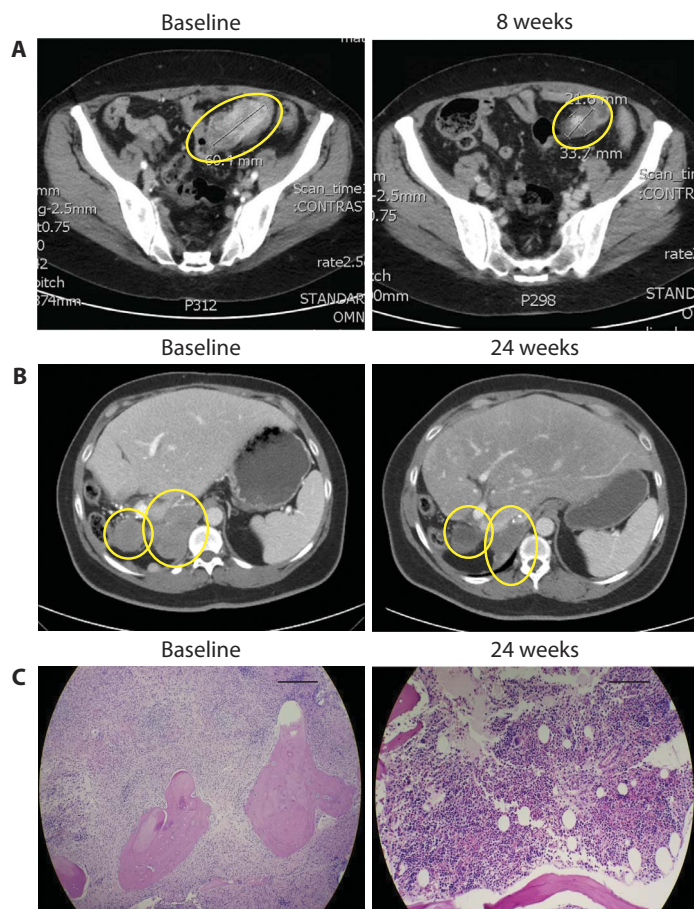


Fig. 5. Clinical data with BLU-285 confirm early evidence of activity in patients with diseases driven by *KIT* and *PDGFRα* activation loop mutations.

(A) BLU-285 (30 mg per os (PO), QD) induces rapid radiographic clinical response per RECIST1.1 (31% tumor reduction at week 8) and decline in *PDGFRα* D842V ctDNA in a patient with *PDGFRα* D842V-mutant GIST that progressed on previous imatinib, dasatinib, and crenolanib therapy. The images show CT scans with tumor circled in yellow. The graph shows tumor burden as measured by the sum of the longest dimension for the target lesions (per RECIST1.1) and mutant allele frequency (MAF). (B) Radiographic clinical response per RECIST1.1 with BLU-285 (60 mg PO, QD) in a patient with primary *KIT* D820Y-mutant GIST that had previously progressed on imatinib, sunitinib, and regorafenib. The images show CT scans with a pelvic tumor mass highlighted within yellow circles that demonstrated a 28% tumor reduction at day 1 of cycle 5. A partial response of 32% tumor reduction was confirmed by central radiographic review at cycle 15. (C) BLU-285 (30 mg PO, QD) markedly decreased bone marrow mast cell burden in a patient with *KIT* D816V-driven aggressive SM. At baseline, diffuse bone marrow infiltration with malignant mast cells obliterated normal hematopoiesis (left). After BLU-285 treatment, there was a marked reduction in malignant mast cells and return of normal trilineage hematopoiesis (right). Scale bars, 1000 μ m (left) and 200 μ m (right).

DISCUSSION

Until now, patients with diseases associated with *KIT* or *PDGFRα* activation loop mutant kinases have had few meaningful treatment options. Drug discovery efforts to address these genetic drivers have primarily focused on repurposing multikinase inhibitors with ancillary *KIT*/*PDGFRα* activity, engineering activation loop mutant activity into imatinib-like type II scaffolds, or developing target-directed antibodies, both naked and conjugated to cytotoxics. Unfortunately, these approaches have all failed to date because of an inability to sufficiently inhibit *KIT* and *PDGFRα* activation loop mutations without concomitant dose-limiting toxicities. With no viable therapeutic options in hand, doctors are left filling this medical void by administering to patients either ineffective drugs or agents whose use lacks sound scientific rationale. For example, many patients with either *PDGFRα* D842V GIST or *KIT* D816V SM receive imatinib despite a mountain of preclinical and clinical data that demonstrate its ineffectiveness. The delivery of such therapies introduces unnecessary risk to patients and increasingly unjustifiable health care expense (39).

BLU-285 was designed as a potent and highly selective inhibitor of *KIT* and *PDGFRα* activation loop mutant kinases. In contrast to the approved type II agents with *KIT* inhibitory activity, BLU-285, a type I inhibitor that binds the active conformation of the kinase, was able to inhibit all activation loop aberrations tested, including the difficult-to-target *PDGFRα* D842V and structurally homologous *KIT* D816V mutants. As anticipated from this precision targeted approach, BLU-285 rapidly demonstrated signs of clinical activity in patients harboring these particular mutations, even at the lowest dose levels tested. On the basis of

these observations, BLU-285 has the potential to address the medical need for these genomically defined patient populations.

Preclinical profiling against numerous *KIT* primary activating mutants and several secondary resistance mutants identified in imatinib- or imatinib/sunitinib-resistant GIST patients demonstrated that BLU-285 maintained activity against a broad spectrum of additional disease-relevant *KIT* mutants, with only slightly shifted potencies both in vitro and in vivo. This is unsurprising, given that the various activating mutations all serve, albeit to differing degrees, to shift the conformational equilibrium of *KIT* to the active form, thus enhancing its affinity for BLU-285. By escalating doses of BLU-285 in ongoing clinical studies in patients with GIST and SM, we will likely be able to determine the extent and spectrum of additional *KIT* and *PDGFRα* activating mutations that can be inhibited adequately to result in meaningful clinical outcomes.

Although the full spectrum of clinical mutants covered by BLU-285 will be characterized with emerging data over time, it may not be feasible for any single inhibitor to address all of the various mutations identified in *KIT* and *PDGFRα* in a kinome-selective manner. In addition, similar to most other targeted therapies against kinase drivers, new on-target resistance mutations may manifest themselves upon prolonged treatment. Although forthcoming clinical trial data will illuminate any gaps that exist in BLU-285 coverage, combination strategies designed to complement or enhance the activity of BLU-285 in oncogenic *KIT*- and *PDGFRα*-driven disease should also be considered. Given the high degree of kinome selectivity and a seemingly favorable clinical safety profile in early trials, BLU-285 is a promising candidate for both

targeted single agent and combination regimens in *KIT*/*PDGFRA*-driven malignancies.

MATERIALS AND METHODS

Study design

The aim of this study was to design and characterize BLU-285, a potent, selective small-molecule inhibitor of *KIT*/*PDGFRA* activating mutants including activation loop mutants. BLU-285 activity was assessed in enzymatic assays with recombinant *KIT*/*PDGFRA* WT or mutant protein, cell lines driven by mutant *KIT* activation, and in vivo pre-clinical *KIT*-driven models. All animal studies were performed under Institutional Animal Care and Use Committee (IACUC) guidelines established at each respective institution where study was conducted. The sample size for animal experiments ($n = 6$ to 11) was based on the results of preliminary experiments, with exact numbers described in Materials and Methods. Mice were randomly assigned to the treatment and control groups; investigators were not blinded during evaluation of the preclinical in vivo experiments. The BLU-285 FIH phase 1 clinical trial was an open-label, nonrandomized study built to assess safety, MTD, pharmacokinetics, pharmacodynamics, and preliminary antitumor activity of BLU-285.

LanthaScreen binding assays

Serially diluted compounds, *KIT* protein, and anti-glutathione *S*-transferase–Europium antibody were incubated with tracer as follows: *KIT* WT, V560G, and D820E proteins with tracer 222 and *KIT* D816E, A829P, and D816V with Tracer 178. Plates were incubated at 25°C for 60 min and read on a PerkinElmer EnVision with two excitation flashes and two emission reads: $\lambda_{\text{ex}} = 350$ nm, $\lambda_{\text{em}} = 665$ nm; $\lambda_{\text{ex}} = 350$ nm, $\lambda_{\text{em}} = 615$ nm.

IC₅₀ generation

Raw data were normalized to 0 and 100% inhibition controls using dimethyl sulfoxide (DMSO) and staurosporine, respectively. IC₅₀ values were calculated using a three- or four-parameter logistic nonlinear regression model.

BLU-285 synthesis

The synthesis of BLU-285 is described in issued patent WO2015/057873; example 7, compound 44.

KINOMEScan binding assays

Compounds were screened at 3 μ M concentration against a panel of 392 WT kinase constructs using the KINOMEScan assay platform at DiscoverX, as previously described (40).

Hotspot kinase profiling assays

In vitro kinase profiling of *KIT* and *PDGFRA* constructs was performed at Reaction Biology Corporation. Kinase/substrate pairs, serially diluted compounds, and any additional cofactors required were prepared in a reaction buffer at their respective Michaelis constant (K_m) for ATP. ³³P-ATP (10 mCi/ml) was added to initiate the reaction, followed by the detection of kinase activity by a filter-binding method.

Cell culture

HMC1.1 and HMC1.2 cell lines were licensed from J. Butterfield (Mayo Clinic) (41). Cells were grown in Iscove's modified Dulbecco's medium containing 20 or 10% fetal calf serum supplemented with iron (HyClone). Kasumi-1, P815, and Chinese hamster ovary (CHO)–K1 cells (American

Type Culture Collection) were grown in vendor-recommended medium. M-07e cells (DSMZ) were grown in Dulbecco's modified Eagle's medium containing granulocyte-macrophage colony-stimulating factor (5 ng/ml) for maintenance or in SCF (5 ng/ml) for cell-based assays. *PDGFRA* WT and mutant kinase constructs were transiently transfected into CHO cells, as previously described (29). All cells underwent short tandem repeat authentication; cells were discarded after 20 passages.

Immunoblot analysis

After treatment of cells with compounds, cells were lysed in Phospho-Safe lysis buffer with protease/phosphatase inhibitors. Total protein concentration was determined using a bicinchoninic acid (BCA) assay (Pierce). Primary antibodies include total *KIT* (#3308, Cell Signaling Technology), pTyr719-*KIT* (#3391, Cell Signaling Technology), total *PDGFRA* (sc-338), pTyr754-*PDGFRA* (sc-12911), total *AKT* (#2920, Cell Signaling Technology), pSer473-*AKT* (#4060, Cell Signaling Technology), total *ERK* (#9107, Cell Signaling Technology), pTyr/Thr 202/204-*ERK* (#4370, Cell Signaling Technology), and β -actin (ab3280, Abcam). Secondary antibodies were from Rockland Antibodies and Assays [IRDye 800–conjugated rabbit immunoglobulin G (IgG) and IRDye 700–conjugated mouse IgG]. Immunoblots were imaged using an Odyssey LI-COR Fluorescent imaging system. *PDGFRA* autophosphorylation was assessed by immunoprecipitation, followed by immunoblotting for phospho-*PDGFRA* and total *PDGFRA*, as previously described (14). To quantitate the percent of p*KIT*/*PDGFR* inhibition in cells, the p*KIT*/total *KIT* ratio was calculated for each concentration of compound and normalized to the average of DMSO-treated cells.

Autophosphorylation assays

AlphaLISA

Cells were seeded in a 384-well plate and incubated overnight at 37°C. Compounds were serially diluted in 100% DMSO, added to cells at a final DMSO concentration of 0.25%, and incubated at 37°C for 90 min. Cells were lysed with AlphaLISA Lysis Buffer supplemented with protease/phosphatase inhibitors with shaking for 30 min at 4°C. Total biotinylated human *KIT* (#3308, Cell Signaling Technology), murine *KIT* (ab112167, Abcam), and phosphoY719-*KIT* (#3391, Cell Signaling Technology) antibodies and AlphaLISA donor and acceptor beads were added to lysates. Plates were read on an EnVision using an AlphaScreen protocol.

Enzyme-linked immunosorbent assay

A PathScan phospho c-kit (panTyr) sandwich enzyme-linked immunosorbent assay (#7294, Cell Signaling Technology) was used to assess the percent inhibition of autophosphorylation of *KIT* WT. M-07e cells were seeded into a 96-well plate in serum/cytokine-free medium, followed by the addition of compounds for 60 min at 37°C. The cells were stimulated with human SCF (50 ng/ml) and scanned on an EnVision plate reader.

Cellular proliferation

Cells were plated in serum-containing medium and incubated overnight at 37°C. Compounds were serially diluted and added to cells at a final DMSO concentration of 0.25% and incubated at 37°C for 72 hours. Cell Titer-Glo reagent was added and read on the EnVision using a 384-well luminescence protocol.

Animal studies

All animal studies were performed under IACUC guidelines established at each respective institution where the study was conducted. BLU-285

was formulated in 0.5% carboxymethyl cellulose + 1% Tween 80. Dasatinib (Selleckchem) was formulated in 50% propylene glycol. Imatinib (Carbosynth) was formulated in sterile water. Regorafenib (Carbosynth) was formulated in a PEG400/125 mM methanesulfonic acid (MSA) mixture at 80:20 ratio. MSA (125 mM) was prepared in water. Sunitinib (Carbosynth) was formulated in 50 mM citrate buffer (pH 3.5). The P815 xenograft study was performed at WuXi AppTec in Shanghai, China. BALB/c nude mice were inoculated with 1×10^6 P815 cells subcutaneously at the right flank. When the average tumor size reached about 75 mm³, treatment with test article began. Ten animals were treated per group. Tumors were measured to assess antitumor activity. For PK/PD analysis, plasma and tumors were collected from three mice per group. The GIST exon 11/17 (model 2007031011) and exon 11/13 (model GS11331) xenograft studies were performed at Crown Biosciences. Nonobese diabetic–severe combined immunodeficient mice were inoculated with 100,000 to 125,000 viable cells subcutaneously into the rear flank. Animals were randomized when average tumor volume reached 150 to 200 mm³, followed by oral dosing of compounds. Eleven animals were treated per group. Plasma and tumor samples were collected from three animals per group. The GIST exon 11 (model UZLX-GIST3) xenograft (42) study was performed in the Laboratory of Experimental Oncology at KU Leuven, Belgium. Tumors were bilaterally implanted onto the rear flanks of adult nude *nu/nu* NMRI mice and randomized upon reaching an average tumor volume of ~500 mm³. Six animals were treated per group for a total of 12 individual tumor measurements. One animal per group was sacrificed for PK/PD analysis, and the other five were used to evaluate antitumor activity.

Xenograft tumor pharmacodynamic analysis

Frozen tumor slices were homogenized in 400 µl of PhosphoSafe lysis buffer with protease/phosphatase inhibitors. Protein concentration was determined using a BCA assay. Fifty micrograms of lysate was subject to SDS–polyacrylamide gel electrophoresis, followed by immunoblotting.

BLU-285 phase 1 study

Open label, nonrandomized, global, FIH phase 1, dose-escalation studies with BLU-285 in advanced, unresectable GIST (NCT02508532) and advanced SM (NCT02561988) were initiated to define the safety, MTD, pharmacokinetics, pharmacodynamics, and preliminary antitumor activity of BLU-285 in each indication. Initial sample size for each study was about 60 patients (25 patients in dose escalation and 35 in dose expansion) as appropriate for FIH studies designed to identify an MTD and assess preliminary antitumor activity. All statistical analyses of safety, pharmacokinetic, pharmacodynamic, and efficacy data were descriptive in nature because the primary objective of the studies was to define the safety and MTD of BLU-285. The studies were reviewed and approved by the institutional review board at each clinical site. Written informed consent was obtained from all patients before study entry. Key eligibility criteria for the GIST study included adult patients (≥ 18 years of age) with unresectable GIST who had received ≥ 2 kinase inhibitors, including imatinib, or patients with tumors bearing a *PDGFRA* D842 mutation regardless of previous therapy; Eastern Cooperative Oncology Group (ECOG) performance status of 0 to 2; and adequate bone marrow, hepatic, renal, and cardiac function. BLU-285 was administered orally, once daily, on a 4-week cycle using a 3 + 3 dose-escalation design. Adverse events per Common Terminology Criteria for Adverse Events (CTCAE), pharmacokinetics, ctDNA levels (Sysmex Inostics), and centrally reviewed radiographic response per

RECIST1.1 were assessed. Presented data are preliminary and represent a cutoff of 28 April 2017. Key eligibility criteria for the advanced SM study included adult patients (≥ 18 years of age) with aggressive SM, SM with associated hematologic neoplasm and one or more C-findings, or mast cell leukemia per World Health Organization diagnostic criteria; ECOG performance status of 0 to 3; and adequate bone marrow, hepatic, renal, and cardiac function. BLU-285 was administered orally, once daily, on a 4-week cycle using a 3 + 3 dose escalation design. Adverse events per CTCAE, pharmacokinetics, ctDNA levels, and markers of mast cell burden, including serum tryptase and bone marrow mast cell content, were assessed. Presented data are preliminary with data cutoff of 1 December 2016.

Statistical analysis

Results for in vivo preclinical models were expressed as mean \pm SEM. Multiple group comparisons were made using Wilcoxon's matched pair test, Mann-Whitney *U* test, or one-way ANOVA, followed by Tukey's multiple comparisons test. *P* < 0.05 was considered statistically significant. Analyses of preliminary efficacy data in the phase 1 BLU-285 clinical trial are descriptive in nature.

SUPPLEMENTARY MATERIALS

www.sciencetranslationalmedicine.org/cgi/content/full/9/414/eaao1690/DC1

Fig. S1. Analysis of compound binding reveals broad type I activity across various forms of KIT.

Fig. S2. BLU-285 inhibits KIT signaling in a KIT exon 11/17 human cell line.

Fig. S3. BLU-285 exhibits differential activity on PDGFRA WT and V561D and D842V mutants.

Fig. S4. Pharmacodynamic analysis of KIT signaling in a P815 allograft model of SM demonstrates in vivo target engagement.

Fig. S5. BLU-285 is well tolerated in a KIT mutant exon 11/17 PDX model of relapsed GIST.

Fig. S6. Histology of GIST PDX KIT mutant exon 11/17 tumors confirms tumor regression.

Fig. S7. Histology of GIST PDX KIT mutant exon 11 tumors was correlated with tumor size regression.

Fig. S8. BLU-285 is well tolerated in a KIT mutant exon 11 PDX model of primary GIST.

Table S1. Human kinases with more than 90% binding by BLU-285, imatinib, sunitinib, regorafenib, crenolanib, and midostaurin are listed.

Table S2. BLU-285 has selectivity for KIT D816V over several kinase antitargets.

Table S3. Antitumor activity of BLU-285 and type II inhibitors across various KIT mutant–driven models of disease highlights robust activity of BLU-285.

REFERENCES AND NOTES

1. C. Zhou, Y.-L. Wu, G. Chen, J. Feng, X.-Q. Liu, C. Wang, S. Zhang, J. Wang, S. Zhou, S. Ren, S. Lu, L. Zhang, C. Hu, C. Hu, Y. Luo, L. Chen, M. Ye, J. Huang, X. Zhi, Y. Zhang, Q. Xiu, J. Ma, L. Zhang, C. You, Erlotinib versus chemotherapy as first-line treatment for patients with advanced *EGFR* mutation-positive non-small-cell lung cancer (OPTIMAL, CTONG-0802): A multicentre, open-label, randomised, phase 3 study. *Lancet Oncol.* **12**, 735–742 (2011).
2. E. L. Kwak, Y.-J. Bang, D. R. Camidge, A. T. Shaw, B. Solomon, R. G. Maki, S.-H. I. Ou, B. J. Dezube, P. A. Jänne, D. B. Costa, M. Varella-Garcia, W.-H. Kim, T. J. Lynch, P. Fidas, H. Stubbs, J. A. Engelman, L. V. Sequist, W. Tan, L. Gandhi, M. Mino-Kenudson, G. C. Wei, S. M. Shreeve, M. J. Ratain, J. Settleman, J. G. Christensen, D. A. Haber, K. Wilner, R. Salgia, G. I. Shapiro, J. W. Clark, A. J. Iafrate, Anaplastic lymphoma kinase inhibition in non-small-cell lung cancer. *N. Engl. J. Med.* **363**, 1693–1703 (2010).
3. A. T. Shaw, S.-H. I. Ou, Y.-J. Bang, D. R. Camidge, B. J. Solomon, R. Salgia, G. J. Riely, M. Varella-Garcia, G. I. Shapiro, D. B. Costa, R. C. Doebele, L. P. Le, Z. Zheng, W. Tan, P. Stephenson, S. M. Shreeve, L. M. Tye, J. G. Christensen, K. D. Wilner, J. W. Clark, A. J. Iafrate, Crizotinib in *ROS1*-rearranged non-small-cell lung cancer. *N. Engl. J. Med.* **371**, 1963–1971 (2014).
4. G. Bollag, P. Hirth, J. Tsai, J. Zhang, P. N. Ibrahim, H. Cho, W. Spevak, C. Zhang, Y. Zhang, G. Habets, E. A. Burton, B. Wong, G. Tsang, B. L. West, B. Powell, R. Shellooe, A. Marimuthu, H. Nguyen, K. Y. J. Zhang, D. R. Artis, J. Schlessinger, F. Su, B. Higgins, R. Iyer, K. D'Andrea, A. Koehler, M. Stumm, P. S. Lin, R. J. Lee, J. Grippo, I. Puzanov, K. B. Kim, A. Ribas, G. A. McArthur, J. A. Sosman, P. B. Chapman, K. T. Flaherty, X. Xu, K. L. Nathanson, K. Nolop, Clinical efficacy of a RAF inhibitor needs broad target blockade in *BRAF*-mutant melanoma. *Nature* **467**, 596–599 (2010).

5. S. G. O'Brien, F. Guilhot, R. A. Larson, I. Gathmann, M. Baccarani, F. Cervantes, J. J. Cornelissen, T. Fischer, A. Hochhaus, T. Hughes, K. Lechner, J. L. Nielsen, P. Rousselot, J. Reiffers, G. Saglio, J. Shepherd, B. Simonsson, A. Gratwohl, J. M. Goldman, H. Kantarjian, K. Taylor, G. Verhoef, A. E. Bolton, R. Capdeville, B. J. Druker, IRIS Investigators, Imatinib compared with interferon and low-dose cytarabine for newly diagnosed chronic-phase chronic myeloid leukemia. *N. Engl. J. Med.* **348**, 994–1004 (2003).
6. G. D. Demetri, M. von Mehren, C. D. Blanke, A. D. Van den Abbeele, B. Eisenberg, P. J. Roberts, M. C. Heinrich, D. A. Tuveson, S. Singer, M. Janicek, J. A. Fletcher, S. G. Silverman, S. L. Silberman, R. Capdeville, B. Kiese, B. Peng, S. Dimitrijevic, B. J. Druker, C. Corless, C. D. M. Fletcher, H. Joensuu, Efficacy and safety of imatinib mesylate in advanced gastrointestinal stromal tumors. *N. Engl. J. Med.* **347**, 472–480 (2002).
7. J. Lennartsson, L. Rönstrand, Stem cell factor receptor/c-Kit: From basic science to clinical implications. *Physiol. Rev.* **92**, 1619–1649 (2012).
8. C. R. Antonescu, P. Besmer, T. Guo, K. Arkun, G. Hom, B. Koryotowski, M. A. Leversha, P. D. Jeffrey, D. Desantis, S. Singer, M. F. Brennan, R. G. Maki, R. P. DeMatteo, Acquired resistance to imatinib in gastrointestinal stromal tumor occurs through secondary gene mutation. *Clin. Cancer Res.* **11**, 4182–4190 (2005).
9. M. C. Barnett, M. C. Heinrich, Management of tyrosine kinase inhibitor-resistant gastrointestinal stromal tumors. *Am. Soc. Clin. Oncol. Educ. Book* **32**, 663–668 (2012).
10. C. R. Antonescu, The GIST paradigm: Lessons for other kinase-driven cancers. *J. Pathol.* **233**, 251–261 (2011).
11. C. D. Blanke, C. Rankin, G. D. Demetri, C. W. Ryan, M. von Mehren, R. S. Benjamin, A. K. Raymond, V. H. C. Bramwell, L. H. Baker, R. G. Maki, M. Tanaka, J. R. Hecht, M. C. Heinrich, C. D. M. Fletcher, J. J. Crowley, E. C. Borden, Phase III randomized, intergroup trial assessing imatinib mesylate at two dose levels in patients with unresectable or metastatic gastrointestinal stromal tumors expressing the kit receptor tyrosine kinase: S0033. *J. Clin. Oncol. Off. J. Am. Soc. Clin. Oncol.* **26**, 626–632 (2008).
12. M. C. Heinrich, R. G. Maki, C. L. Corless, C. R. Antonescu, A. Harlow, D. Griffith, A. Town, A. McKinley, W.-B. Ou, J. A. Fletcher, C. D. M. Fletcher, X. Huang, D. P. Cohen, C. M. Baum, G. D. Demetri, Primary and secondary kinase genotypes correlate with the biological and clinical activity of sunitinib in imatinib-resistant gastrointestinal stromal tumor. *J. Clin. Oncol.* **26**, 5352–5359 (2008).
13. B. Liehl, J. Kepten, C. Le, M. Zhu, G. D. Demetri, M. C. Heinrich, C. D. M. Fletcher, C. L. Corless, J. A. Fletcher, Heterogeneity of kinase inhibitor resistance mechanisms in GIST. *J. Pathol.* **216**, 64–74 (2008).
14. M. C. Heinrich, C. L. Corless, A. Duensing, L. McGreevey, C.-J. Chen, N. Joseph, S. Singer, D. J. Griffith, A. Haley, A. Town, G. D. Demetri, C. D. M. Fletcher, J. A. Fletcher, *PDGFRA* activating mutations in gastrointestinal stromal tumors. *Science* **299**, 708–710 (2003).
15. S. Hirota, A. Ohashi, T. Nishida, K. Isozaki, K. Kinoshita, Y. Shinomura, Y. Kitamura, Gain-of-function mutations of platelet-derived growth factor receptor α gene in gastrointestinal stromal tumors. *Gastroenterology* **125**, 660–667 (2003).
16. P. A. Cassier, E. Fumagalli, P. Rutkowski, P. Schöffski, M. Van Glabbeke, M. Debiec-Rychter, J.-F. Emile, F. Duffaud, J. Martin-Broto, B. Landi, A. Adenis, F. Bertucci, E. Bompas, O. Bouché, S. Leyvraz, I. Judson, J. Verweij, P. Casali, J.-Y. Blay, P. Hohenberger, European Organisation for Research and Treatment of Cancer, Outcome of patients with platelet-derived growth factor receptor α -mutated gastrointestinal stromal tumors in the tyrosine kinase inhibitor era. *Clin. Cancer Res.* **18**, 4458–4464 (2012).
17. M. C. Heinrich, C. L. Corless, G. D. Demetri, C. D. Blanke, M. von Mehren, H. Joensuu, L. S. McGreevey, C.-J. Chen, A. D. Van den Abbeele, B. J. Druker, B. Kiese, B. Eisenberg, P. J. Roberts, S. Singer, C. D. M. Fletcher, S. Silberman, S. Dimitrijevic, J. A. Fletcher, Kinase mutations and imatinib response in patients with metastatic gastrointestinal stromal tumor. *J. Clin. Oncol. Off. J. Am. Soc. Clin. Oncol.* **21**, 4342–4349 (2003).
18. C. Yoo, M.-H. Ryu, J. Jo, I. Park, Y.-Y. Ryoo, Y.-K. Kang, Efficacy of imatinib in patients with platelet-derived growth factor receptor α -mutated gastrointestinal stromal tumors. *Cancer Res. Treat.* **48**, 546–552 (2016).
19. T. Kristensen, H. Vestergaard, M. B. Møller, Improved detection of the *KIT* D816V mutation in patients with systemic mastocytosis using a quantitative and highly sensitive real-time qPCR assay. *J. Mol. Diagn.* **13**, 180–188 (2011).
20. A. C. Garcia-Montero, M. Jara-Acevedo, C. Teodosio, M. L. Sanchez, R. Nunez, A. Prados, I. Aldanondo, L. Sanchez, M. Dominguez, L. M. Botana, F. Sanchez-Jimenez, K. Sotlar, J. Almeida, L. Escribano, A. Orfao, *KIT* mutation in mast cells and other bone marrow hematopoietic cell lineages in systemic mast cell disorders: A prospective study of the Spanish Network on Mastocytosis (REMA) in a series of 113 patients. *Blood* **108**, 2366–2372 (2006).
21. A. Pardanani, T. L. Reeder, T. K. Kimlinger, J. Y. Baek, C.-Y. Li, J. H. Butterfield, A. Tefferi, *Flt-3* and *c-kit* mutation studies in a spectrum of chronic myeloid disorders including systemic mast cell disease. *Leuk. Res.* **27**, 739–742 (2003).
22. J. Gotlib, H. C. Kluijn-Nelemans, T. I. George, C. Akin, K. Sotlar, O. Hermine, F. T. Awan, E. Hexner, M. J. Mauro, D. W. Sternberg, M. Villeneuve, A. Huntsman Labed, E. J. Stanek, K. Hartmann, H.-P. Horny, P. Valent, A. Reiter, Efficacy and safety of midostaurin in advanced systemic mastocytosis. *N. Engl. J. Med.* **374**, 2530–2541 (2016).
23. J. Zhang, P. L. Yang, N. S. Gray, Targeting cancer with small molecule kinase inhibitors. *Nat. Rev. Cancer* **9**, 28–39 (2009).
24. C. D. Mol, D. R. Dougan, T. R. Schneider, R. J. Skene, M. L. Kraus, D. N. Scheibe, G. P. Snell, H. Zou, B.-C. Sang, K. P. Wilson, Structural basis for the autoinhibition and STI-571 inhibition of c-Kit tyrosine kinase. *J. Biol. Chem.* **279**, 31655–31663 (2004).
25. C. D. Mol, K. B. Lim, V. Sridhar, H. Zou, E. Y. T. Chien, B.-C. Sang, J. Nowakowski, D. B. Kassel, C. N. Cronin, D. E. McRee, Structure of a c-Kit product complex reveals the basis for kinase transactivation. *J. Biol. Chem.* **278**, 31461–31464 (2003).
26. K. S. Gajiwala, J. C. Wu, J. Christensen, G. D. Deshmukh, W. Diehl, J. P. DiNitto, J. M. English, M. J. Greig, Y.-A. He, S. L. Jacques, E. A. Lunney, M. McTigue, D. Molina, T. Quenzer, P. A. Wells, X. Yu, Y. Zhang, A. Zou, M. R. Emmett, A. G. Marshall, H.-M. Zhang, G. D. Demetri, KIT kinase mutants show unique mechanisms of drug resistance to imatinib and sunitinib in gastrointestinal stromal tumor patients. *Proc. Natl. Acad. Sci. U.S.A.* **106**, 1542–1547 (2009).
27. C. L. Corless, C. M. Barnett, M. C. Heinrich, Gastrointestinal stromal tumours: Origin and molecular oncology. *Nat. Rev. Cancer* **11**, 865–878 (2011).
28. E. Ben Ami, G. D. Demetri, A safety evaluation of imatinib mesylate in the treatment of gastrointestinal stromal tumor. *Expert Opin. Drug Saf.* **15**, 571–578 (2016).
29. M. C. Heinrich, D. Griffith, A. McKinley, J. Patterson, A. Presnell, A. Ramachandran, M. Debiec-Rychter, Crenolanib inhibits the drug-resistant *PDGFRA* D842V mutation activating with imatinib-resistant gastrointestinal stromal tumors. *Clin. Cancer Res.* **18**, 4375–4384 (2012).
30. M. Sundström, H. Vliagoftis, P. Karlberg, J. H. Butterfield, K. Nilsson, D. D. Metcalfe, G. Nilsson, Functional and phenotypic studies of two variants of a human mast cell line with a distinct set of mutations in the *c-kit* proto-oncogene. *Immunology* **108**, 89–97 (2003).
31. S. Demehri, A. Corbin, M. Loriaux, B. J. Druker, M. W. Deininger, Establishment of a murine model of aggressive systemic mastocytosis/mast cell leukemia. *Exp. Hematol.* **34**, 284–288 (2006).
32. A. Beghini, I. Magnani, C. B. Ripamonti, L. Larizza, Amplification of a novel c-Kit activating mutation Asn⁸²²-Lys in the Kasumi-1 cell line: A t(8;21)-Kit mutant model for acute myeloid leukemia. *Hematol. J.* **3**, 157–163 (2002).
33. M. M. Schittenhelm, S. Shiraga, A. Schroeder, A. S. Corbin, D. Griffith, F. Y. Lee, C. Bokemeyer, M. W. N. Deininger, B. J. Druker, M. C. Heinrich, Dasatinib (BMS-354825), a dual SRC/ABL kinase inhibitor, inhibits the kinase activity of wild-type, juxtamembrane, and activation loop mutant KIT isoforms associated with human malignancies. *Cancer Res.* **66**, 473–481 (2006).
34. S. Verstovsek, A. Tefferi, J. Cortes, S. O'Brien, G. Garcia-Manero, A. Pardanani, C. Akin, S. Faderl, T. Manshour, D. Thomas, H. Kantarjian, Phase II study of dasatinib in Philadelphia chromosome-negative acute and chronic myeloid diseases, including systemic mastocytosis. *Clin. Cancer Res.* **14**, 3906–3915 (2008).
35. T. Van Looy, Y. K. Gebreyohannes, A. Wozniak, J. Cornillie, J. Wellens, H. Li, U. Vanleeuw, G. Floris, M. Debiec-Rychter, R. Sciôt, P. Schöffski, Characterization and assessment of the sensitivity and resistance of a newly established human gastrointestinal stromal tumour xenograft model to treatment with tyrosine kinase inhibitors. *Clin. Sarcoma Res.* **4**, 10 (2014).
36. H. Joensuu, P. J. Roberts, M. Sarlomo-Rikala, L. C. Andersson, P. Tervahartiala, D. Tuveson, S. L. Silberman, R. Capdeville, S. Dimitrijevic, B. Druker, G. D. Demetri, Effect of the tyrosine kinase inhibitor STI571 in a patient with a metastatic gastrointestinal stromal tumor. *N. Engl. J. Med.* **344**, 1052–1056 (2001).
37. M. C. Heinrich, R. L. Jones, M. von Mehren, P. Schöffski, S. Bauer, O. Mir, P. A. Cassier, F. Eskens, H. Shi, T. Alvarez-Diez, O. Schmidt-Kittler, M. E. Healy, B. B. Wolf, S. George, Clinical activity of BLU-285 in advanced gastrointestinal stromal tumor (GIST). *J. Clin. Oncol. Off. J. Am. Soc. Clin. Oncol.* **35**, 11011 (2017).
38. M. W. Drummond, D. J. DeAngelo, M. W. Deininger, D. Radia, A. T. Quiery, E. O. Hexner, H. Shi, T. Alvarez-Diez, E. K. Evans, M. E. Healy, B. B. Wolf, S. Verstovsek, Preliminary safety and clinical activity in a phase 1 study of BLU-285, a potent, highly-selective inhibitor of KIT D816V in Advanced Systemic Mastocytosis (SM). *Blood* **128**, 477 (2016).
39. P. Schöffski, A. Wozniak, O. Schöffski, L. van Eycken, M. Debiec-Rychter, Overcoming cost implications of mutational analysis in patients with gastrointestinal stromal tumors: A pragmatic approach. *Oncol. Res. Treat.* **39**, 811–816 (2016).
40. M. I. Davis, J. P. Hunt, S. Herrgard, P. Ciceri, L. M. Wodicka, G. Pallares, M. Hocker, D. K. Treiber, P. P. Zarrinkar, Comprehensive analysis of kinase inhibitor selectivity. *Nat. Biotechnol.* **29**, 1046–1051 (2011).
41. J. H. Butterfield, D. Weiler, G. Dewald, G. J. Gleich, Establishment of an immature mast cell line from a patient with mast cell leukemia. *Leuk. Res.* **12**, 345–355 (1988).
42. T. Van Looy, A. Wozniak, G. Floris, R. Sciôt, H. Li, J. Wellens, U. Vanleeuw, J. A. Fletcher, P. W. Manley, M. Debiec-Rychter, P. Schöffski, Phosphoinositide 3-kinase inhibitors combined with imatinib in patient-derived xenograft models of gastrointestinal stromal tumors: Rationale and efficacy. *Clin. Cancer Res.* **20**, 6071–6082 (2014).

Acknowledgments: We thank our colleagues at Blueprint Medicines for the thoughtful discussions and constructive feedback throughout the course of the BLU-285 program and for the critical review of the manuscript. We also thank the scientists at WuXi AppTec and CrownBio for their excellent in vivo study support and execution, A. Tsimboukis for the graphic design contributions, and all of the patients and their families, the doctors, and the nurses for their participation in the ongoing phase 1 clinical trials with BLU-285. **Funding:** This work was funded by Blueprint Medicines. In addition, contributions from the Heinrich laboratory were funded, in part, by a VA Merit Review grant (2I01BX000338-05) to M.C.H. **Author contributions:** E.K.E., A.K.G., J.L.K., and C.L. wrote and revised the manuscript. A.S. performed the enzymatic binding and activity assays. A.K.G., A.D., and X.J.Z. performed the cellular assays. B.L.H., D.W., K.W., L.D., Y.Z., J.L.K., N.B., N.L., and T.G. contributed to the design and synthesis of BLU-285. J.L.K. and N.B. provided the structural biology and computational chemistry insights to support BLU-285 generation. E.K.E., A.K.G., N.K., A.W., Y.K.G., and P.S. designed and performed the in vivo xenograft studies. T.P.L. and Y.K.G. performed immunohistochemistry analysis. M.C.H. contributed to the target engagement studies in CHO cells. A.B. and B.W. led the BLU-285 clinical trial design. D.J.D., P.S., and M.C.H. cared for the patients on BLU-285 trial. S.M. and O.S.-K. analyzed ctDNA from the clinical samples. **Competing interests:**

E.K.E., A.K.G., J.L.K., B.L.H., A.D., X.J.Z., O.S.-K., D.W., K.W., N.B., T.P.L., S.M., B.W., T.G., N.L., A.B., and C.L. are current employees and shareholders of Blueprint Medicines. N.L. is a shareholder of Blueprint Medicines. Y.Z., B.L.H., J.L.K., K.W., and D.W. are inventors on patent WO2015/057873 held by Blueprint Medicines, which includes BLU-285. All other authors declare that they have no competing interests.

Submitted 23 June 2017

Accepted 2 October 2017

Published 1 November 2017

10.1126/scitranslmed.aao1690

Citation: E. K. Evans, A. K. Gardino, J. L. Kim, B. L. Hodous, A. Shutes, A. Davis, X. J. Zhu, O. Schmidt-Kittler, D. Wilson, K. Wilson, L. DiPietro, Y. Zhang, N. Brooijmans, T. P. LaBranche, A. Wozniak, Y. K. Gebreyohannes, P. Schöffski, M. C. Heinrich, D. J. DeAngelo, S. Miller, B. Wolf, N. Kohl, T. Guzi, N. Lydon, A. Boral, C. Lengauer, A precision therapy against cancers driven by *KIT/PDGFR*A mutations. *Sci. Transl. Med.* **9**, eaao1690 (2017).

A precision therapy against cancers driven by *KIT*/*PDGFRA* mutations

Erica K. Evans, Alexandra K. Gardino, Joseph L. Kim, Brian L. Hodous, Adam Shutes, Alison Davis, Xing Julia Zhu, Oleg Schmidt-Kittler, Doug Wilson, Kevin Wilson, Lucian DiPietro, Yulian Zhang, Natasja Brooijmans, Timothy P. LaBranche, Agnieszka Wozniak, Yemarshet K. Gebreyohannes, Patrick Schöffski, Michael C. Heinrich, Daniel J. DeAngelo, Stephen Miller, Beni Wolf, Nancy Kohl, Timothy Guzi, Nicholas Lydon, Andy Boral and Christoph Lengauer

Sci Transl Med **9**, eaao1690.
DOI: 10.1126/scitranslmed.aao1690

Treatment makes tumors feel BLU

Mutations in receptor tyrosine kinases are common in cancer, and a variety of kinase mutations can have oncogenic effects. Not all of these mutations are susceptible to existing kinase inhibitors, and many inhibitors are nonspecific, resulting in undesirable off-target effects. Evans *et al.* developed BLU-285, an inhibitor that specifically targets the KIT and PDGFRA oncogenic kinases. The authors showed that the compound is very specific for its targets, can inhibit them in the presence of multiple oncogenic mutations, and is selective for the mutant forms of the kinases relative to the wild type. In addition to biochemical and preclinical testing of BLU-285, the authors conducted a phase 1 study, which showed evidence of the compound's activity in human cancer patients.

ARTICLE TOOLS

<http://stm.sciencemag.org/content/9/414/eaao1690>

SUPPLEMENTARY MATERIALS

<http://stm.sciencemag.org/content/suppl/2017/10/30/9.414.eaao1690.DC1>

RELATED CONTENT

<http://stm.sciencemag.org/content/scitransmed/7/318/318ra202.full>
<http://stm.sciencemag.org/content/scitransmed/6/259/259ra145.full>
<http://stm.sciencemag.org/content/scitransmed/6/268/268ra177.full>

REFERENCES

This article cites 42 articles, 13 of which you can access for free
<http://stm.sciencemag.org/content/9/414/eaao1690#BIBL>

PERMISSIONS

<http://www.sciencemag.org/help/reprints-and-permissions>

Use of this article is subject to the [Terms of Service](#)